



## Snowball versus slushball Earth: Dynamic versus nondynamic sea ice?

J. P. Lewis,<sup>1</sup> A. J. Weaver,<sup>1</sup> and M. Eby<sup>1</sup>

Received 29 November 2006; revised 8 June 2007; accepted 14 August 2007; published 21 November 2007.

[1] Modeling studies of the Neoproterozoic snowball Earth offer two variations for snowball conditions, the original “hard” snowball Earth where the ocean is completely covered by sea ice, and an alternate slushball Earth or “soft” snowball, where there is an equatorial oasis of open water. We use the University of Victoria Earth System Climate Model to show that the soft snowball result is only possible when dynamics are excluded from the sea ice component of the model. Using a purely thermodynamic sea ice component the soft snowball condition is stable, whereas with a dynamic and thermodynamic sea ice component it is not. As the behavior of dynamic sea ice largely depends on wind stress, we compare simulations using two different wind fields: a zonally averaged present-day wind field and a wind field derived by a general circulation model, the Fast Ocean Atmosphere Model, using Neoproterozoic conditions. Another consequence of using dynamic sea ice is that the sea ice does not become sufficiently thick to flow under its own weight when there is open water; this suggests that sea glacier dynamics are not important for snowball inception.

**Citation:** Lewis, J. P., A. J. Weaver, and M. Eby (2007), Snowball versus slushball Earth: Dynamic versus nondynamic sea ice?, *J. Geophys. Res.*, 112, C11014, doi:10.1029/2006JC004037.

### 1. Introduction

[2] The original snowball Earth theory was proposed to explain the formation of shallow marine, equatorial glacial deposits during the Neoproterozoic (1000–542 Ma) [Kirschvink, 1992; Hoffman *et al.*, 1998]. Now sometimes referred to as the ‘hard’ snowball Earth, the original theory suggested that the oceans must have been covered with sea ice from the poles to the equator [Kirschvink, 1992]. It was suggested that, with most of the continental mass near the equator, higher equatorial albedo and CO<sub>2</sub> drawdown due to enhanced silicate weathering, lead to global cooling and sea ice expanding equatorward from the polar latitudes [Hoffman and Schrag, 2002]. Once the sea ice reached a critical latitude of ~30° the powerful snow/ice albedo feedback caused further rapid cooling, freezing over the remaining open ocean. The Earth would have remained in a frozen state until millions of years of volcanic outgassing built up a greenhouse effect strong enough to melt back the sea ice, resulting in hot house conditions [Hoffman *et al.*, 1998]. Although the hard snowball theory proposed to explain other anomalous deposits such as ‘cap carbonates’, banded iron formations and isotope anomalies, there was much resistance to the theory as it was thought to be too extreme for the survival of eukaryotes and could not account for the evidence of open water during glacial deposition. An

alternative theory was proposed by Hyde *et al.* [2000], now deemed the slushball, or ‘soft’ snowball Earth.

[3] Using the GENESIS 2 general circulation model (GCM) with a fixed continental ice sheet, Hyde *et al.* [2000] concluded that it was possible for sea ice to extend from the poles to only ~25° latitude, satisfying the condition for complete continental glaciation and yet leaving an equatorial oasis for the survival of eukaryotes [Hyde *et al.*, 2000]. Other modeling studies, which did not result in continental glaciation at the equator, did find that a low-latitude sea ice margin was stable, with sea ice extending to within ~25° latitude of the equator [Chandler and Sohl, 2000; Baum and Crowley, 2001; Crowley *et al.*, 2001; Poulsen and Jacob, 2004]. The thin sea ice scenario proposed by McKay [2000] was found to be unrealistic by Warren *et al.* [2002] owing to the simple broadband model used in calculating the absorption depth of the sea ice. None of the previous experiments investigated the effects of dynamic sea ice, that is, sea ice that can be transported by wind and ocean currents.

[4] Surface wind speed and wind stress on the ocean during the Neoproterozoic would have typically been highest in the midlatitudes, with an average eastward direction, similar to present day [Poulsen and Jacob, 2004]. As will be discussed below, midlatitude sea ice would have felt a net force toward the equator by the westerly wind stress and the Coriolis effect. The equatorward movement of sea ice may have made an equatorial oasis under Neoproterozoic conditions implausible. Here results are presented from a sensitivity study in which simulations were conducted under different wind and CO<sub>2</sub> conditions in order to

<sup>1</sup>School of Earth and Ocean Sciences, University of Victoria, Victoria, British Columbia, Canada.

examine the influence of sea ice dynamics on snowball inception.

## 2. Model

[5] All experiments conducted in this study use version 2.7 of the University of Victoria (UVic) Earth System Climate Model (ESCM) [Weaver *et al.*, 2001]. The model consists of a 3-D ocean GCM (Modular Ocean Model 2.2) coupled to a thermodynamic/dynamic sea ice model and an energy-moisture balance atmosphere model. The ocean component of the coupled model is a fully nonlinear 3-D ocean GCM [Pacanowski, 1995] with a global resolution of a  $3.6^\circ$  (zonal) by  $1.8^\circ$  (meridional) and 19 vertical levels. The thermodynamic sea ice model used in this study has a simple two-category thickness distribution [Hibler, 1979; Parkinson and Washington, 1979; Semtner, 1976] while the dynamic component incorporates an elastic-viscous-plastic rheology [Hunke and Dukowicz, 1997]. Atmospheric heat transport is accomplished through Fickian diffusion while moisture transport occurs through both advection and diffusion. Precipitation occurs when the relative humidity exceeds 90%. Precipitation over land instantaneously returns to the ocean as a line source along the coastline unless it falls as snow, in which case it is locally retained until it melts or is sublimated. The atmospheric model includes a parametrization of water vapor-planetary long-wave feedbacks [Thompson and Warren, 1982]. The model resolves the annual cycle and the incoming solar radiation at the top of the atmosphere depends on the orbital parameters [Berger, 1978].

[6] For the suite of sensitivity experiments we used an idealized supercontinent centered on the equator with a uniform 50 m elevation. The solar luminosity was reduced from present day by 6% [Endal and Sofia, 1981], the rotation rate of the Earth was increased to represent a Neoproterozoic 18-hour day [Hyde *et al.*, 2000; Jenkins and Smith, 1999] and a  $50 \text{ m W m}^{-2}$  geothermal flux was added uniformly to the bottom of the ocean [Adcroft *et al.*, 2001]. For better comparison with other studies, the orbital parameters were kept at present day values. Sea ice albedo was 0.5 while snow albedo was 0.75 with a snow masking depth of 25 cm.

[7] Owing to the simple atmosphere, an external wind field must be imposed for the UVic model. There are three components to the wind field: surface wind speed is used in the calculation of surface fluxes; wind stress acts upon the ocean surface and sea ice; and weighted vertically integrated winds are used for the advection of moisture [Weaver *et al.*, 2001]. The surface wind speed and wind stress are interpolated from the lowest level of a 3-D atmospheric data set while the wind for moisture advection is derived by vertically integrating the data set after it has been weighted by the vertical profile of specific humidity at each grid point. The weighting tends to favor winds in the boundary layer where specific humidity is normally greatest.

[8] For this study, wind fields were derived from two different data sets. The first wind field (PD) was derived from NCEP data of the present day southern hemisphere [Kalnay *et al.*, 1996] with wind fields being annually and zonally averaged, then reflected across the equator to produce a meridionally symmetric wind field. The present

day southern hemisphere was chosen because of the strong pole to equator temperature gradient and the lack of mid-latitude landmasses, similar to Neoproterozoic conditions.

[9] The second wind field (Neo) was derived from a Neoproterozoic simulation using the Fast Ocean Atmosphere Model v1.5 (FOAM). The atmosphere component is based on the CCM3 and has a global resolution of a  $2.8^\circ$  (zonal) by  $1.4^\circ$  (meridional) and 18 levels [Poulsen and Jacob, 2004]. For a complete description of the FOAM model see Jacob [1997]. The FOAM experiment that produced the wind data set used in this study was an ice free experiment that had an idealized continent at the equator and high levels of  $\text{CO}_2$  that provided a relatively weak pole to equator temperature gradient (R. T. Pierrehumbert, personal communication, 2006). The Neo wind field was derived from monthly averages once the experiment reached equilibrium. Because of the weak meridional temperature gradient, the 'Neo' wind field probably represents the weakest likely winds for snowball inception. Once sea ice formed at the poles and moved equatorward, the meridional temperature gradient would increase and the wind strength would increase accordingly [Donnadieu *et al.*, 2004; Poulsen and Jacob, 2004].

[10] The 'PD' and 'Neo' wind fields, derived from data with very different pole to equator temperature gradients, represent good starting points for conducting a sensitivity study of Neoproterozoic wind fields; the Neo wind field representing initial ice free conditions and the PD wind field representing conditions where sea ice extended to the mid latitudes.

[11] In order to examine the influence of sea ice dynamics on the initiation of snowball conditions, a suite of experiments were conducted with and without sea ice dynamics, using both wind fields. These initially ice-free experiments were started from rest and integrated until quasiequilibrium, typically 3000–6000 years. Experiments using dynamic sea ice where the ocean did not completely freeze over reached equilibrium while those that froze over completely reached a quasiequilibrium where sea ice thickness continued to increase. Experiments using nondynamic sea ice reached a quasiequilibrium where the latitude of the sea ice margin stabilized but the ice thickness continued to grow, especially near the poles. It was not computationally feasible for all experiments to reach equilibrium as in many experiments the sea ice thickness would eventually grow to  $\sim 1000 \text{ m}$ , balanced only by the geothermal heat flux. Experiments were conducted over a broad range of  $\text{CO}_2$  concentrations, starting at 500 ppm and increasing by 500 ppm until snowball inception no longer occurred, with additional experiments conducted near inception thresholds. For both wind fields, only experiments near the snowball inception thresholds are shown.

## 3. Results and Discussion

### 3.1. Neo Wind Field

[12] Comparing the Neo wind field with and without sea ice dynamics (Figure 1), it is evident that the inclusion of sea ice dynamics has a significant effect on the sea ice margin equilibrium latitude over a broad range of  $\text{CO}_2$  levels, with the dynamic sea ice leading to a hard snowball solution at higher levels of  $\text{CO}_2$ . At  $\text{CO}_2$  concentrations

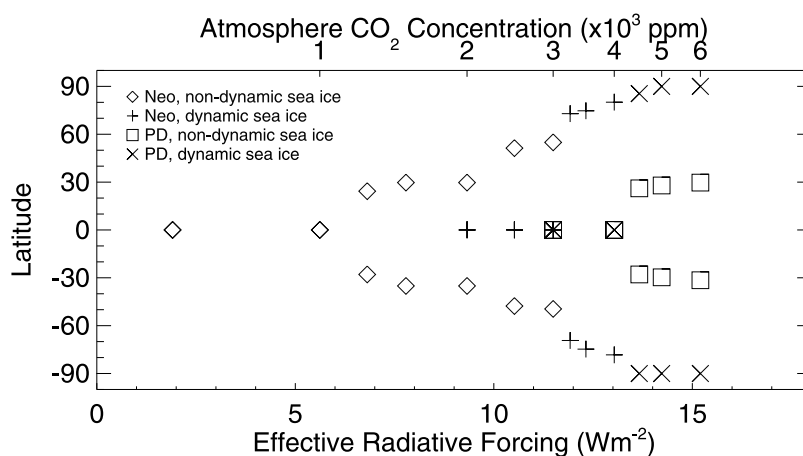


**Figure 1.** Quasiequilibrium conditions for experiments using the Neo and PD wind fields with dynamic and nondynamic sea ice. Symbols at 0° latitude represent “hard” snowball conditions (similar to Figure 2a), symbols between ~30° and 0° represent “soft” snowball conditions where there is an equatorial oasis of open water and yet the continent accumulates sufficient snow cover to initiate glaciation at the equator (similar to Figure 2b), and symbols > ~30° represent nonsnowball conditions where there is not sufficient snow cover on the continent to initiate glaciation (similar to Figure 2c).

below ~3000 ppm the dynamic sea ice experiments result in completely ice covered oceans while with an additional ~0.5 W m<sup>-2</sup> of CO<sub>2</sub> forcing, the sea ice margin stabilizes at ~70°, a considerable jump compared to the nondynamic sea ice experiment. With only the thermodynamic sea ice component, the hard snowball solution exists up to ~1000 ppm CO<sub>2</sub>. At slightly higher CO<sub>2</sub> concentrations, the sea ice margin moves poleward but is still stable within the tropics and the continent has sufficient snow cover for glacial inception at the equator, creating an oasis solution (Figure 2). At CO<sub>2</sub> concentrations greater than ~2500 ppm the continent no longer becomes glaciated. For clarity, the oasis solution is considered a separate solution from the open water solution because equatorial glaciation on the continent is initiated. As such, with nondynamic sea ice, there are three stable solutions, a hard snowball solution, a nonsnowball solution and an intermediate soft snowball solution with an equatorial oasis of open water (Figure 2). The soft snowball solution does not appear to be stable with the inclusion of sea ice dynamics.

[13] These results compare favorably to the study by *Poulsen and Jacob* [2004] where, using the FOAM model with a thermodynamic sea ice component and excluding the radiative effect of clouds, their experiment resulted in global sea ice cover at 140 ppm CO<sub>2</sub>. As they were investigating a number of other sensitivities they did not conduct experiments at higher CO<sub>2</sub> levels which makes a more direct comparison difficult. The lack of atmosphere dynamics and the radiative effects of clouds may make simulations in this study more prone to snowball conditions [*Poulsen and Jacob*, 2004].

[14] Clouds have both a warming effect, owing to their absorption and reradiation of outgoing longwave radiation, and a cooling effect caused by their relatively high albedo reflecting incoming solar radiation away from the surface. The net effect depends on cloud height as well as the albedo of the surface below it. Over ice and snow, the cooling effect of clouds is reduced as a result of the diminished

contrast between the cloud albedo and the surface albedo [*Pierrehumbert*, 2002]. Therefore, over ice and snow during the Neoproterozoic, clouds would have had a predominantly warming effect that may have inhibited snowball inception [*Pierrehumbert*, 2005; *Poulsen and Jacob*, 2004]. As *Poulsen and Jacob* [2004] demonstrated, the effects of clouds play an important role in modeling snowball conditions, but the magnitude and sign of the forcing during the Neoproterozoic is obviously uncertain, as it is in present day. The FOAM model yields an increase in global cloud cover compared to present day when modeling snowball conditions [*Poulsen et al.*, 2001], while similar experiments using the GENESIS v2.0 GCM yield a 35% reduction [*Hyde et al.*, 2000]. In light of these large uncertainties, it is constructive to investigate the role of sea ice dynamics excluding cloud feedbacks.

### 3.2. PD Wind Field

[15] The PD wind field resulted in hard snowball conditions at higher CO<sub>2</sub> levels when compared to the Neo wind field and in all PD experiments with CO<sub>2</sub> levels below 4000 ppm, sea ice cover was global (Figure 1). At higher CO<sub>2</sub> levels, the results were similar to those with the Neo wind field in that using dynamic sea ice resulted in only two stable equilibrium conditions, the hard snowball and nonsnowball states. Increasing the CO<sub>2</sub> forcing by ~0.5 W m<sup>-2</sup> above 4000 ppm resulted in the sea ice margin stabilizing at ~85°. Again, excluding sea ice dynamics allowed for a third condition, the soft snowball, with the sea ice margin stable in the tropics and equatorial glaciation on the continent. A consistent result of all experiments was that the soft snowball condition was only possible when sea ice dynamics were excluded, regardless of CO<sub>2</sub> level and wind field.

[16] Comparing the PD and Neo wind fields in Figure 1 shows that the effect of excluding sea ice dynamics was not consistent between the two wind fields. When sea ice dynamics were included using the Neo wind field, experiments were more likely to result in snowball conditions. For

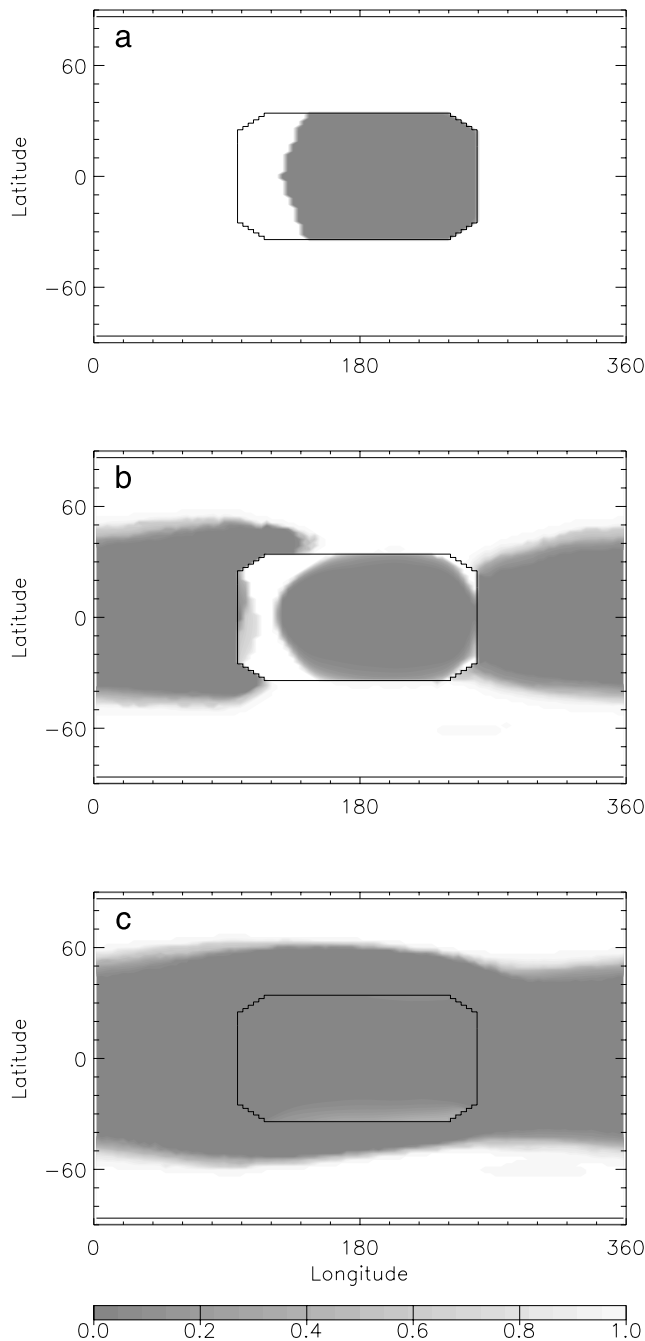


**Figure 2.** Annual average snow/ice area at quasiequilibrium using the Neo wind field and nondynamic sea ice for CO<sub>2</sub> concentrations of (a) 1000 ppm, (b) 2000 ppm, and (c) 3000 ppm. These are representative examples of a “hard” snowball solution with completely ice covered oceans (Figure 2a), a “soft” snowball solution with open water and continental glaciation at the equator (Figure 2b), and a nonsnowball solution with no equatorial glaciation on the continent (Figure 2c).

the PD wind field, warmer conditions resulted when using dynamic sea ice. To further examine the role of the winds on snowball inception, experiments were conducted to determine the relative effect of each wind component: surface wind speed, wind stress and wind for moisture advection.

### 3.3. Comparing Wind Components

[17] Using both dynamic and nondynamic sea ice, a set of experiments was conducted exchanging wind components between the PD and Neo wind fields at 3000 ppm CO<sub>2</sub> (Table 1). Figure 3 shows the equilibrium latitude of the sea ice margin for the 16 experiments in Table 1. 3000 ppm CO<sub>2</sub> was chosen for the comparison concentration as, at that level, the Neo wind field with dynamic sea ice resulted in hard snowball conditions while the nondynamic sea ice did not. Perturbing the wind field by changing wind components at that sensitive level would likely result in different outcomes and provide insight into the relative effects of the wind fields. The CO<sub>2</sub> level could have been chosen at a higher value where the PD wind field results differed between dynamic and nondynamic sea ice but the equilibrium differences were not as distinct as for the Neo wind field.

#### 3.3.1. Surface Wind Speed

[18] Surface wind speed had the most influence on the amount of CO<sub>2</sub> required to achieve a hard snowball condition. All eight experiments with the PD surface wind speed (exp: 1, 3, 4, 7, 9, 11, 12, 15) resulted in hard snowball conditions compared to only two using the Neo surface wind speed (exp: 5, 8). To further investigate the effect of the surface wind speed, two more experiments were conducted using a 50% reduction in the PD surface wind speed, with and without sea ice dynamics (not shown). Similar to simulation results under Neo surface wind speed conditions (exp: 2, 10), the adoption of reduced PD surface wind speed resulted in nonsnowball conditions for dynamic sea ice, although nondynamic sea ice resulted in soft snowball conditions. The global average surface wind speeds of the reduced PD surface wind speed and the Neo surface wind speed were the same, 3.8 m s<sup>-1</sup>, but there were differences in the zonal strengths (Figure 4).

[19] The calculation of sensible and latent heat are both linearly dependent on surface wind speed. All else being equal, doubling the surface wind speed doubles the sensible heat exchange between the ocean and atmosphere and doubles the latent heat loss due to evaporation. For Neoproterozoic conditions, the atmosphere is almost always colder than the ocean and an increase in surface wind speed acts to cool the surface ocean facilitating sea ice growth. Higher average surface wind speed was the main reason why experiments using the PD winds resulted in hard snowball conditions at higher CO<sub>2</sub> levels when compared to the Neo wind simulations, however, surface wind speed cannot explain why the response to sea ice dynamics was not consistent between the two wind fields.

#### 3.3.2. Wind Stress

[20] The effect of changing wind stress was only apparent in dynamic sea ice experiments using the Neo surface wind speed and did not depend on which moisture advection component was used (Table 1). All of the experiments using Neo surface wind speed and nondynamic sea ice (exp: 10, 13, 14, 16) regardless of wind stress, resulted in nonsnowball conditions with the sea ice margin stabilizing at ~45° latitude (Figure 3). Comparing the dynamic sea ice experiments 2 or 6 (PD wind stress) and 8 or 5 (Neo wind stress), the Neo wind stress was conducive to hard snowball conditions whereas the PD wind stress was not. A main difference between the two wind stress fields was the

**Table 1.** Quasiequilibrium Conditions for Experiments Using 3000 ppm CO<sub>2</sub><sup>a</sup>

Experiment Number, Dynamic/Nondynamic	Equilibrium Result, Dynamic/Nondynamic	PD			Neo		
		Wind Speed	Wind Stress	Moisture Advection	Wind Speed	Wind Stress	Moisture Advection
1/9	hard/hard	Y	Y	Y	N	N	N
2/10	no/no	N	Y	Y	Y	N	N
3/11	hard/hard	Y	Y	N	N	N	Y
4/12	hard/hard	Y	N	Y	N	Y	N
5/13	hard/no	N	N	N	Y	Y	Y
6/14	no/no	N	Y	N	Y	N	Y
7/15	hard/hard	Y	N	N	N	Y	Y
8/16	hard/no	Y	Y	Y	N	N	N

<sup>a</sup>Dynamic/nondynamic denotes type of sea ice; “Y” indicates that the wind component specified at the top of the column was used in the experiment, and “N” indicates that it was not; “hard” indicates completely ice covered oceans (similar to Figure 2a), and “no” indicates that sea ice did not extend into the tropics (similar to Figure 2c).

magnitude of the stresses (Figure 5). The PD wind stress was much larger in both the zonal and meridional directions, especially in the mid latitudes where its direct effect on sea ice would be greatest. The dynamic sea ice at those latitudes was transported toward the equator regardless of the wind field used.

[21] Intuitively the stronger wind stress should extend the sea ice margin further equatorward. This was not the case (Figure 6); the effect of wind stress on the dynamic sea ice was not as important as the effect of the wind stress on ocean circulation and its meridional heat transport. Owing to the greater PD wind stress, sea ice was transported equatorward more rapidly, resulting in thinner sea ice that was more easily melted by the increased ocean heat transport, preventing the equatorward advance of the sea ice margin and inhibiting hard snowball conditions. Comparing dynamic sea ice thickness for the two wind stresses supports these conclusions. For a similar sea ice extent, the average dynamic sea ice thickness using the PD wind stress (exp: 6) was  $\sim 13$  cm while using the Neo wind stress (exp: 5) the average sea ice thickness was  $\sim 56$  cm. This result was mirrored when using nondynamic sea ice; the PD wind stress (exp: 14) yielded an average sea ice thickness of  $\sim 21$  m while the weaker Neo wind stress (exp: 13) had an average sea ice thickness of  $\sim 36$  m. The stronger PD wind stress consistently produced more poleward ocean heat transport to the sea ice margin, resulting in thinner sea ice that was unable to extend as far equatorward as experiments using the Neo wind stress (Figure 6).



**Figure 3.** Equilibrium ice line latitudes for the 16 experiments in Table 1. The ice line latitude corresponds to the center of each number. The order of the experiments has been artificially changed to progress the ice line from the equator to the poles to make it easier to compare scenarios; the particular order is irrelevant.

[22] It should be noted that the temporal sequence in Figure 6 is not representative in any way of the actual Neoproterozoic evolution of climate states toward a snowball Earth. It would have taken many thousands to several million years for CO<sub>2</sub> to slowly decrease and the sea ice margin to advanced through the mid to low latitudes. It is solely used here to illustrate the interactions between sea ice dynamics and wind stress.

### 3.3.3. Moisture Advection

[23] For the present study, moisture advection had the least impact on simulation results. Comparing open water scenarios with Neo moisture advection (exp: 14, 13, 6) to the equivalent scenarios using PD moisture advection (exp: 10, 16, 2), it can be clearly seen from Figure 3 that the difference in moisture advection had little effect. The magnitude of the PD moisture advection was greater for both the zonal and meridional components compared to the Neo moisture advection (Figure 7). Both zonal components were of similar magnitude in the tropics but of opposite sign. Owing to the symmetry of the geography, the difference in sign would have only switched the side of the continent where precipitation was predominantly deposited. The Neo moisture advection scenarios deposited precipitation on the East side of the continent while precipitation in the PD moisture advection scenarios was deposited on the western side.

### 3.4. Dynamic Versus Nondynamic Sea Ice

[24] Wind stress, and its associated meridional ocean heat transport, accounted for the fact that the Neo wind field resulted in snowball conditions at higher CO<sub>2</sub> levels with

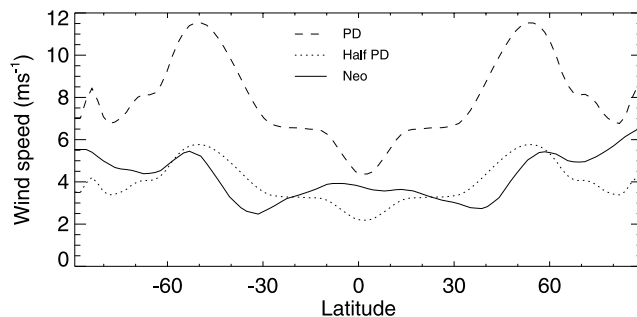


**Figure 4.** Annual zonal average surface wind speed from the PD and Neo wind fields.

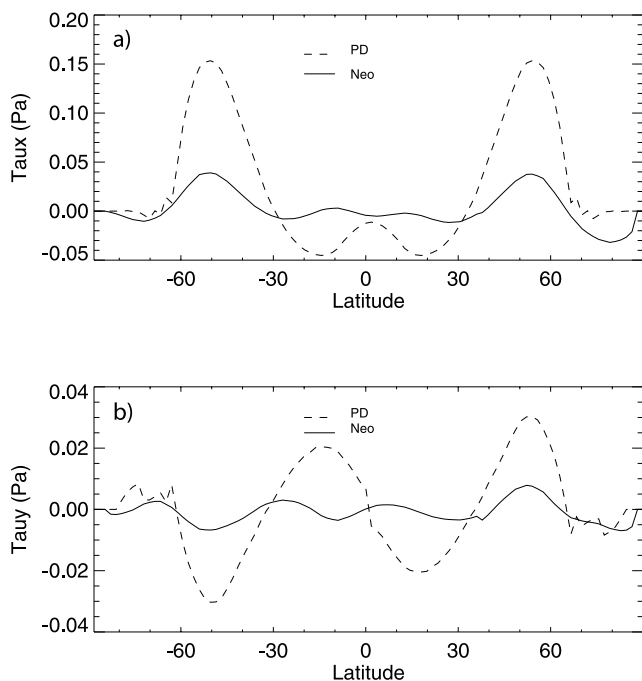


**Figure 5.** Annual zonal average wind stress in the (a) eastward ( $T_{aux}$ ) and (b) northward ( $T_{auy}$ ) direction from the PD and Neo wind fields.

sea ice dynamics than with nondynamic sea ice, in contrast to using the PD wind field. The effect of wind stress on dynamic sea ice simulations was greater than for nondynamic sea ice owing to their relative thicknesses. Purely thermodynamic sea ice was on the order of tens of meters thick (and growing) while dynamic sea ice was only centimeters thick. The limited amount of thermal inertial in the thin sea ice meant that the magnitude of ocean heat transport had a much greater effect on the dynamic sea ice than on the thick, nondynamic sea ice.

[25] Further comparison of experiments with dynamic sea ice versus nondynamic sea ice showed that all experiments with dynamic sea ice, regardless of wind field, were initially (after 500 years) warmer than the equivalent nondynamic sea ice experiments and that the dynamic sea ice did not

extend as far equatorward (Figure 6). Even the Neo experiments that resulted in hard snowball conditions were initially warmer than the equivalent nondynamic sea ice experiments that did not freeze over. For the Neo hard snowball experiments the dynamic sea ice extent surpassed that of the nondynamic sea ice prior to the critical latitude for the runaway albedo feedback, consequently freezing over the remaining ocean, while the nondynamic sea ice margin remained at a stable latitude (Figure 6). This was not seen using the PD wind field, the purely thermodynamic sea ice extent was always greater than in similar simulations using dynamic sea ice.

[26] To visualize the effect of wind stress between dynamic and nondynamic sea ice experiments, it is constructive to examine the four experiments in Figure 6 at year 2000. The nondynamic sea ice experiment with weaker wind stress (exp. 13) has a sea ice margin latitude of  $\sim 40^\circ$ . The equivalent dynamic sea ice experiment (exp. 5) has a sea ice margin slightly equatorward of the nondynamic sea ice margin. Increasing the wind stress increases the meridional ocean heat transport and moves the nondynamic sea ice margin slightly poleward to  $\sim 45^\circ$  latitude (exp. 14), a difference of  $\sim 5^\circ$ . For the dynamic sea ice experiment, increasing the wind stress has a much greater effect because the dynamic sea ice is much thinner and its sea ice margin moves poleward a greater distance to  $\sim 55^\circ$  latitude (exp. 6), a difference of  $\sim 15^\circ$ .

[27] The magnitude of the PD wind stress was such that the nondynamic sea ice always extended equatorward of the dynamic sea ice. Incrementally reducing the wind stress would have narrowed the distance between the two sea ice margins until the wind stress was reduced to a point where the two sea ice margins were at the same latitude. Further reducing the wind stress would result in the dynamic sea ice margin extending equatorward of the nondynamic sea ice margin. The Neo wind stress was weak enough for the dynamic sea ice margin to extend equatorward of the nondynamic sea ice margin, explaining the opposing effects of including sea ice dynamics into the Neo and PD snowball simulations in Figure 1.

[28] Nondynamic sea ice was stable to lower latitudes than dynamic sea ice, as seen by comparing the stable nondynamic sea ice extent in Figure 2b to the unstable dynamic sea ice in the top image of Figure 8. Figure 8

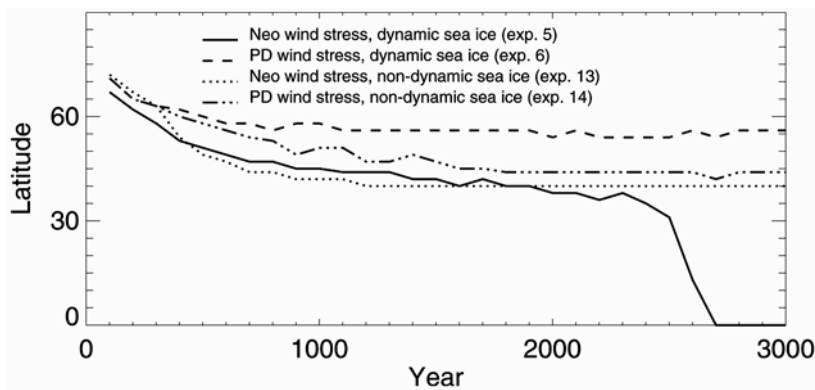


**Figure 6.** Time series of minimum sea ice margin latitude for experiments at 3000 ppm  $CO_2$  using Neo surface wind speed and moisture advection (experiments 5, 6, 13, and 14 in Table 1). The data were plotted at 100-year intervals.

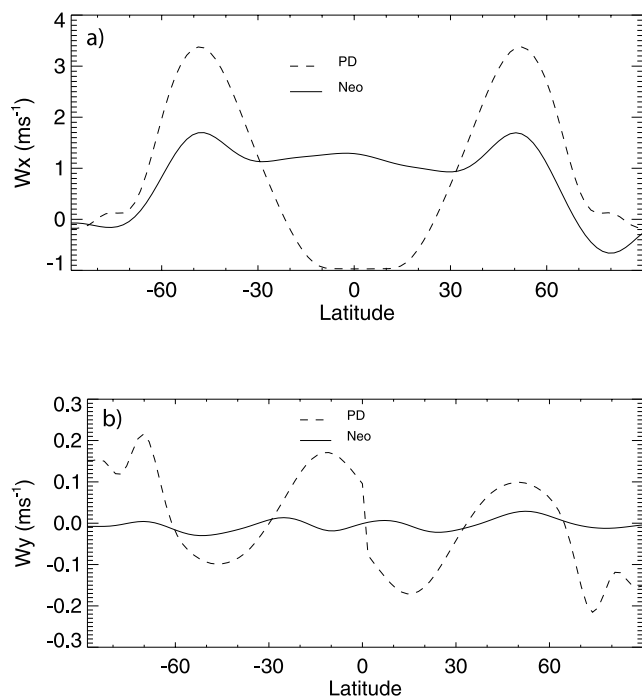


**Figure 7.** Annual zonal average wind for moisture advection in the (a) eastward ( $W_x$ ) and (b) northward ( $W_y$ ) direction from the PD and Neo wind fields.

captures the runaway albedo feedback and rapid transition of experiment 5 into a hard snowball condition. After  $\sim 2500$  years, the dynamic sea ice of experiment 5 reached the critical latitude for runaway albedo feedback, which with our model configuration and albedo values was  $\sim 35^\circ$  latitude for dynamic sea ice (Figure 6). Once sea ice extended past the critical latitude, the transition to hard snowball conditions required less than 150 years. This transition was enhanced by increased continental snow cover (increased albedo) and dynamic sea ice being transported equatorward by the midlatitude westerlies. As the dynamic sea ice extended to the equator, meridional ocean heat transport was weakened and eventually eliminated once the ocean became completely covered in ice. The nondynamic sea ice in Figure 2b did not have the added equatorward transport provided by the wind stress and so was stable even with the sea ice margin near  $\sim 35^\circ$  latitude.

### 3.5. Sea Glacier Dynamics

[29] Recent studies by *Goodman and Pierrehumbert* [2003] and *Pollard and Kasting* [2005] examined the effects of sea glacier fluid dynamics on snowball inception. The sea glacier dynamics resulted in thick polar sea ice deforming plastically under its own weight and flowing equatorward. As the results of the current study clearly indicate, the inclusion of sea ice dynamics would prevent the sea ice from growing sufficiently thick to flow under its own weight until after the ocean became completely ice covered. Stresses by the ocean and atmosphere (wind) transport sea ice equatorward before the ice becomes thick enough for sea glacier dynamics to play a significant role. In the present study, all experiments with dynamic sea ice, that did not

result in snowball conditions, had a maximum equilibrium sea ice thickness of less than 5 m. The sea glacier dynamics would have come into play with the purely thermodynamic sea ice but as nondynamic sea ice is unrealistic, we chose not to include it.

[30] The sea glacier dynamics of *Goodman and Pierrehumbert* [2003] and *Pollard and Kasting* [2005] would, however, become important once the ocean became completely ice covered. With sea ice extending from the pole to the equator, it would essentially be ‘locked up’ and the ocean and atmosphere stresses would no longer be able to transport the sea ice. This would effectively result in purely thermodynamic sea ice growth until the ice became sufficiently thick for sea glacier dynamics to become effective.

## 4. Conclusions

[31] Using the UVic ESCM, the soft snowball condition of an equatorial oasis of open water, with continental

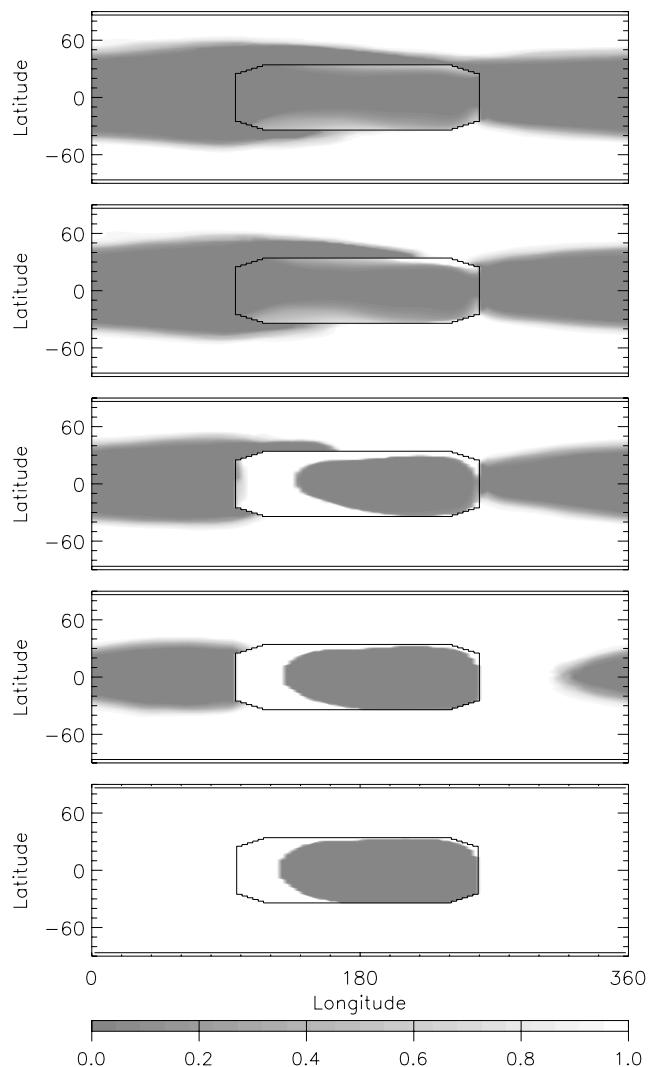


**Figure 8.** Annual average snow/ice area for experiment 5 (Neo wind field at 3000 ppm  $\text{CO}_2$ ) starting at year 2560 at the top and increasing by 20 years to 2640 at the bottom.

glaciation at the equator, was only stable when using a purely thermodynamic sea ice component. When sea ice dynamics were included, the sea ice margin was only stable with a large open ocean (nonsnowball conditions) or with a completely ice covered ocean (hard snowball conditions). These results occurred under two very different wind fields suggesting that the equatorial oasis of open water may not be a plausible solution. Perhaps a soft snowball condition with dynamic sea ice could be stable with a dynamic atmosphere and the radiative effect of clouds, but this has yet to be investigated.

[32] Surface wind speed had a significant influence on the level of CO<sub>2</sub> required to produce a hard snowball solution. Experiments with a global average surface wind speed of 3.8 m s<sup>-1</sup> produced hard snowball conditions at up to 3000 ppm CO<sub>2</sub>, whereas doubling the surface wind speed allowed hard snowball conditions to form at CO<sub>2</sub> levels as high as 4000 ppm. The sensitivity to surface wind speed was due to the sensible and latent heat loss from the ocean, which both linearly depend on surface wind speed. Both the PD and Neo winds transported high and midlatitude sea ice toward the equator. Increasing the wind stress resulted in thinner sea ice transported equatorward more rapidly and increased the meridional ocean heat transport which melted the thin sea ice and inhibited snowball conditions.

[33] This study was not able to determine whether the inclusion of sea ice dynamics would make future experiments more or less likely to produce hard snowball conditions compared to using purely thermodynamic sea ice, as it would depend on the wind stress. A robust result of including dynamic sea ice, however, regardless of wind combination, was that the soft snowball condition of an equatorial oasis was not stable. The inclusion of sea ice dynamics also negates the need for sea glacier dynamics when simulating snowball inception, as dynamic sea ice does not become sufficiently thick to flow under its own weight when there is open water. Once the ocean becomes completely ice covered, the sea glacier dynamics of Goodman and Pierrehumbert [2003] and Pollard and Kasting [2005] would become important for determining the thickness of equatorial sea ice and possibly the fate of photosynthetic eukaryotes.

[34] **Acknowledgments.** We would like to thank Ray Pierrehumbert for invaluable discussions and for providing wind data used in this study. We are grateful for funding from NSERC and the Canadian Foundation for Climate and Atmospheric Sciences. We would also like to thank two anonymous reviewers for their helpful comments and suggestions. This research was made possible through support to A. J. W. from the Canada Research Chair program, and through support to JPL via an NSERC fellowship.

## References

Adcroft, A., J. Scott, and J. Marotzke (2001), Impact of geothermal heating on the global ocean circulation, *Geophys. Res. Lett.*, **28**, 1735–1738.  
 Baum, S., and T. Crowley (2001), GCM response to late Precambrian (~590 Ma) ice-covered continents, *Geophys. Res. Lett.*, **28**, 583–586.  
 Berger, A. (1978), Long-term variations of daily insolation and Quaternary climate change, *J. Atmos. Sci.*, **35**, 2362–2367.

Chandler, M., and L. Sohl (2000), Climate forcing and the initiation of low-latitude ice sheets during the Neoproterozoic Varanger glacial interval, *J. Geophys. Res.*, **105**, 20,737–20,756.  
 Crowley, T., W. Hyde, and W. Peltier (2001), CO<sub>2</sub> levels required for the deglaciation of a “Near-Snowball” Earth, *Geophys. Res. Lett.*, **28**, 283–286.  
 Donnadieu, Y., G. Ramstein, F. Fluteau, D. Roche, and A. Ganopolski (2004), The impact of atmospheric and oceanic heat transports on the sea-ice-albedo instability during the neoproterozoic, *Clim. Dyn.*, **22**, 293–306.  
 Endal, A., and S. Sofia (1981), Rotation in soar-type stars, I, evolutionary models for the spin-down of the Sun, *Astrophys. J.*, **243**, 625–640.  
 Goodman, J., and R. Pierrehumbert (2003), Glacial flow of floating marine ice in “Snowball Earth,” *J. Geophys. Res.*, **108**(C10), 3308, doi:10.1029/2002JC001471.  
 Hibler, I. (1979), A dynamic thermodynamic sea ice model, *J. Phys. Oceanogr.*, **9**, 815–846.  
 Hoffman, P., and D. Schrag (2002), The snowball Earth hypothesis: Testing the limits of global change, *Terra Nova*, **14**, 129–155.  
 Hoffman, P., A. Kaufman, G. Halverson, and D. Schrag (1998), A Neoproterozoic snowball Earth, *Science*, **281**, 1342–1346.  
 Hunke, E., and J. Dukowicz (1997), An elastic-viscous-plastic model for sea ice dynamics, *J. Phys. Oceanogr.*, **27**, 1849–1867.  
 Hyde, W., T. Crowley, S. Baum, and W. Peltier (2000), Neoproterozoic ‘snowball Earth’ simulations with a coupled climate/ice-sheet model, *Nature*, **405**, 425–429.  
 Jacob, R. (1997), Low frequency variability in a simulated atmosphere ocean system, Ph.D. thesis, 159 pp., Univ. of Wis., Madison.  
 Jenkins, G., and S. Smith (1999), GCM simulations of snowball Earth conditions during the late Proterozoic, *Geophys. Res. Lett.*, **26**, 2263–2266.  
 Kalnay, E., et al. (1996), The NCEP/NCAR 40 year reanalysis project, *Bull. Am. Meteorol. Soc.*, **77**, 437–471.  
 Kirschvink, J. (1992), Late Proterozoic low-latitude global glaciation: The snowball Earth, in *The Proterozoic Biosphere: A Multidisciplinary Study*, edited by J. Schopf and C. Klein, pp. 51–52, Cambridge Univ. Press, Cambridge, U. K.  
 McKay, C. (2000), Thickness of tropical ice and photosynthesis on a Snowball Earth, *Geophys. Res. Lett.*, **27**, 2153–2156.  
 Pacanowski, R. (1995), MOM 2: Documentation user’s guide and reference manual, Tech. Rep. 3, 232 pp., GFDL Ocean Group, Princeton, N. J.  
 Parkinson, C., and W. Washington (1979), A large-scale numerical model of sea ice, *J. Geophys. Res.*, **84**, 311–337.  
 Pierrehumbert, R. (2002), The hydrologic cycle in deep-time climate problems, *Nature*, **419**, 191–198.  
 Pierrehumbert, R. T. (2005), Climate dynamics of a hard snowball Earth, *J. Geophys. Res.*, **110**, D01111, doi:10.1029/2004JD005162.  
 Pollard, D., and J. Kasting (2005), Snowball Earth: A thin-ice solution with flowing sea glaciers, *J. Geophys. Res.*, **110**, C07010, doi:10.1029/2004JC002525.  
 Poulsen, C., and R. Jacob (2004), Factors that inhibit snowball Earth simulation, *Paleoceanography*, **19**, PA4021, doi:10.1029/2004PA001056.  
 Poulsen, C., R. Raymond, T. Pierrehumbert, and R. Jacob (2001), Impact of ocean dynamics on the simulation of the Neoproterozoic “snowball Earth”, *Geophys. Res. Lett.*, **28**, 1575–1578.  
 Semtner, A. (1976), A model for the thermodynamic growth of sea ice in numerical investigations of climate, *J. Phys. Oceanogr.*, **6**, 379–389.  
 Thompson, S., and S. Warren (1982), Parameterization of outgoing infrared radiation derived from detailed radiative calculations, *J. Atmos. Sci.*, **39**, 2667–2680.  
 Warren, S. G., R. E. Brandt, T. C. Grenfell, and C. P. McKay (2002), Snowball Earth: Ice thickness on the tropical ocean, *J. Geophys. Res.*, **107**(C10), 3167, doi:10.1029/2001JC001123.  
 Weaver, A., et al. (2001), The UVic Earth System Climate Model: Model description, climatology, and applications to past, present and future climates, *Atmos. Ocean*, **107**(4), 361–428.

M. Eby, J. P. Lewis, and A. J. Weaver, School of Earth and Ocean Sciences, University of Victoria, ISC 294, Stn CSC, PO Box 3055, Victoria, BC, Canada V8W 3P6. (jplewis@uvic.ca)